

Flexural wave band gaps in locally resonant elastic metamaterial plates using Reissner-Mindlin theory

Ferreira, Anderson¹, Dos Santos, José¹, Miranda Jr.², Edson², Nobrega, Edilson³, Ramos, R.⁴

^{1,3}University of Campinas - UNICAMP-FEM-DMC, Rua Mendeleev, 200 Campinas - SP, 13083-860, Brazil.

² Federal Institute of Maranhão, IFMA-EIB-DE, Rua Afonso Pena, 174 São Luís - MA, 65010-030, Brazil.

⁴ University of São Paulo - USP-IF, R. do Matão, 1371 - Butantã, São Paulo - SP, 05508-090, Brazil.

Abstract: The authors present a study of the propagation of flexural waves in a locally resonant (LR) elastic metamaterial made of a two-dimensional periodic array of spring-mass resonators attached on a thick homogeneous plate. The well-known plane wave expansion method (PWE) is extended to deal with such a plate system with a periodic array of lumped resonant elements. Explicit matrix formulations are developed for the calculation of band structures to quantify the wave attenuation performance of band gaps. Modal analysis and forced response are computed by finite element method. The final objective is to show that the two methods agree with one another with the relation of wave attenuation in periodic structures.

Keywords: Elastic Metamaterial thick plate, Flexural wave band gaps, Vibration control.

INTRODUCTION

One of the most important problems in engineering noise and vibration control is the determination of the acoustic and vibration energy transmitted through structures. Elastic wave propagation in periodic systems has been studied a long time ago (Brillouin,53),(Mead,75), and it is well known that such systems present an important feature of filtering waves. Thus, elastic waves cannot propagate freely through periodic structures within some frequency ranges, which are called band gaps. These band gaps are based on the Bragg scattering mechanism (Sigalas,92), whose frequency location is governed by the Bragg's law, *i.e.*, $d = n(\lambda/2)$, $n = 1, 2, 3, \dots$, where d is the lattice constant of periodic system, and λ is the wavelength in host material. Bragg's law implies spatial modulation of the same order as the wavelength, which means difficulties to achieve low frequency band gaps for small size systems. More recently a resonance-type band gap was obtained in frequency bands two orders of magnitude lower than the Bragg limit. Proposed by Liu *et al.* (Liu,2000), it is a metamaterial containing a crystal or structure including attached periodic arrays of local resonators. The investigation of locally resonant metamaterials has been extended to a newly emerging field of acoustic metamaterials. Metamaterial plate including attached low-frequency resonators is a promising solution to obtain light weight acoustic filters. These systems work better to control structural wave propagation (Oudich,2010). Acoustic waves propagation using metamaterial plate for noise reduction using local resonators was investigated theoretically by Xiao *et al.* (Xiao,2012s). In the present work, a thick plate with periodically attached multiple arrays of spring-mass resonators is modelled using the plane wave expansion (PWE) method together with Reissner-Mindlin's thick plate theory. The PWE is extended to treat such a periodic plate system containing lumped resonant elements, and to calculate the imaginary part of the Bloch wave vectors that can be used to quantify the attenuation performance of band gaps. Unlike Kirchoff's thin plate, the Reissner-Mindlin's thick plate takes into account shearing of cross sections and rotational inertia. Results indicate that the different plate theories as Kirchoff and Mindlin can produce quite distinct behavior (Norris,2003). So the bending wave equation (thin plate) must be modified for thick plates to include terms that account for shear deformation and rotatory inertia. The bending wave effectively becomes a combination of pure bending waves and transverse shear waves. For a better understanding of the vibration modes of the structure, finite element simulation results such as modal analysis, forced response as a function of frequency is presented. After obtaining the results of the harmonic analysis by the finite element method, a transmittance graph is presented along with the dispersion curve to analyze the vibration behavior of the structure in a range of 0 to 2 kHz.

1 MODEL AND FORMULATIONS

1.1 The Band Structure

Consider an infinitely homogeneous thick plate in the $x - y$ plane with periodically attached spring-mass resonators, as sketched in Figure 1. In Figure 1 each resonator is composed by a set of N_o independent springs with elastic constants k_j and masses m_j , which determine multiple resonant frequencies, $f_j = (1/2\pi)(k_j/m_j)^{1/2}$. Damping is included as a complex stiffness, $k_j(1 - i\eta_j)$, where η_j is the loss factor. These N_o independent resonators are periodically attached in

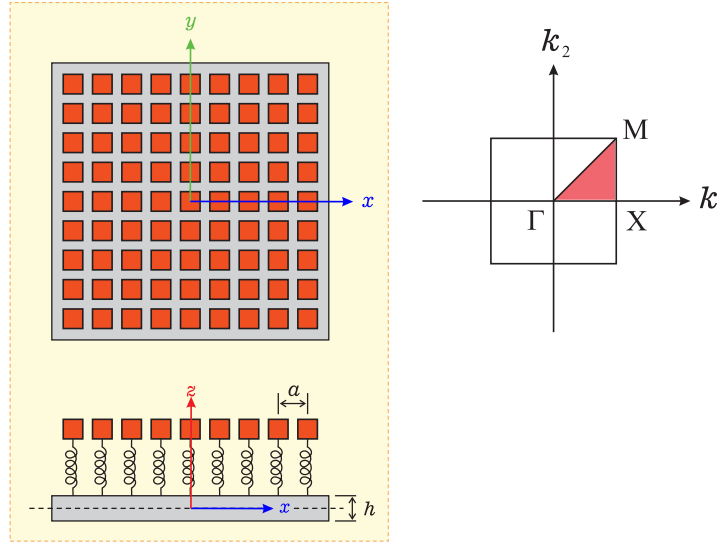


Figure 1 – Top of view schematic diagram of a LR thick plate with a 2D periodic array of attached spring mass resonators. Square lattice and the red area is the irreducible region of the Brillouin Zone. $\Gamma = (0,0)$, $X = (\pi/a,0)$ and $M = (\pi/a,\pi/a)$, are the higher symmetry points in the reciprocal space.

the direct lattice places indexed by:

$$\mathbf{R} = n_1 \mathbf{a}_1 + n_2 \mathbf{a}_2$$

where n_1 and n_2 are integers and $\mathbf{a}_1 = (a,0)$, $\mathbf{a}_2 = (0,a)$ are basis vectors of the direct lattice. The linear system of $3 + N_o$ differential equations governing out of plane harmonic vibration of a plate coupled to the lattice of resonators are obtained based on the classical theory of Reissner-Mindlin thick plate (Szilard,2004). The governing equation for the time-harmonic vibration of the plate-resonator coupled system Figure 1 can be written as:

$$\begin{cases} \frac{D}{2} \left[(1-\nu) \nabla^2 \psi_x(\mathbf{r}) + (1+\nu) (\partial_x \partial_y \psi_y(\mathbf{r}) + \partial_x^2 \psi_x(\mathbf{r})) \right] + \kappa_1^2 Gh (\partial_x w(\mathbf{r}) - \psi_x(\mathbf{r})) - \rho \omega^2 I_p \psi_x(\mathbf{r}) = 0 \\ \frac{D}{2} \left[(1-\nu) \nabla^2 \psi_y(\mathbf{r}) + (1+\nu) (\partial_x \partial_y \psi_x(\mathbf{r}) + \partial_y^2 \psi_y(\mathbf{r})) \right] + \kappa_1^2 Gh (\partial_y w(\mathbf{r}) - \psi_y(\mathbf{r})) - \rho \omega^2 I_p \psi_y(\mathbf{r}) = 0 \\ Gh \kappa_1^2 [\nabla^2 w_1(\mathbf{r}) + \partial_x \psi_x(\mathbf{r}) + \partial_y \psi_y(\mathbf{r})] - \omega^2 \rho h w(\mathbf{r}) = -\sum_{\mathbf{R}} \sum_{j=1}^{N_o} f_j(\mathbf{R}) \delta(\mathbf{r} - \mathbf{R}) \\ -\omega^2 m_j w_j(\mathbf{R}) = f_j(\mathbf{R}) \end{cases} \quad (1)$$

Where $w(\mathbf{r})$, $\psi_x(\mathbf{r})$ and $\psi_y(\mathbf{r})$ are the vertical displacement and angles of rotations at the mid-plane around x and y directions, respectively; $D = Eh^3/12(1-\nu^2)$ represents the plate bending rigidity; h is the plate thickness; ω is the angular frequency; $I_p = h^3/12$; E , G , κ^2 , ρ and ν are Young's modulus of elasticity, shear modulus, shear correction factor, mass density and Poisson's ratio, respectively. $w_j(\mathbf{R})$ is the displacement of the j -th independent resonator attached to the plate at \mathbf{R} position. Damping is included as a complex Young's modulus, $E(1+i\eta_p)$, where η_p is the material plate loss factor.

In the summation term of Eq. (1), $f_j(\mathbf{R})$ is the resonator force applied to the plate located at \mathbf{R} , and $\delta(\mathbf{r} - \mathbf{R})$ is the 2D delta function defined by:

$$\delta(\mathbf{r} - \mathbf{R}) = \delta(x - \mathbf{R}_x) \delta(y - \mathbf{R}_y). \quad (2)$$

The total force intensity, $\sum_{j=1}^{N_o} f_j(\mathbf{R})$, acting on the plate at each lattice position is described in terms of Hooke's law, Eq. (3):

$$\sum_{j=1}^{N_o} f_j(\mathbf{R}) = \sum_{j=1}^{N_o} k_j [w(\mathbf{R}) - w_j(\mathbf{R})], \quad (3)$$

The analytical formulation here adopted follows closely the approach of Xiao *et al.* on Ref. (Xiao,2012s) to Kirchoff's model, however by adopting here the set of Reissner-Mindlin's equation, which includes the torsional degree of freedom of middle plane of the plate, then our modeled plate has an extra internal coupling which is absent in the Xiao's model. The assumed periodicity of the system in the $x-y$ plane can be used to expand the displacement fields of the plate in Fourier series. In addition by imposing also the Floquet-Bloch form to describe the propagating waves in the structure we write the following equations:

$$\psi_x(\mathbf{r}) = \sum_{\mathbf{G}} \Psi_{x,\mathbf{G}} e^{-i(\mathbf{k}+\mathbf{G})\cdot\mathbf{r}}, \quad (4)$$

$$\psi_y(\mathbf{r}) = \sum_{\mathbf{G}} \Psi_{y,\mathbf{G}} e^{-i(\mathbf{k}+\mathbf{G})\cdot\mathbf{r}}, \quad (5)$$

$$w(\mathbf{r}) = \sum_{\mathbf{G}} W_{\mathbf{G}} e^{-i(\mathbf{k}+\mathbf{G})\cdot\mathbf{r}}, \quad (6)$$

where $\mathbf{k} = (k_x, k_y)$ is Bloch wave vector (wave number), and $\mathbf{G} = (G_x, G_y)$ run over the set of N reciprocal-lattice vector used in the Fourier expansion given by:

$$\mathbf{G} = n_1 \mathbf{b}_1 + n_2 \mathbf{b}_2, \quad (7)$$

where n_1, n_2 are integers varying in $\{-n, -n+1, \dots, -1, 0, 1, \dots, n\}$ (where n is an positive integer). Therefore $N = (2n+1)^2$ plane waves are used in the Fourier expansion of plate displacements. The reciprocal-lattice basis vectors are $\mathbf{b}_1 = (b_{11}, b_{12})$ and $\mathbf{b}_2 = (b_{21}, b_{22})$ are defined as $\mathbf{a}_p \cdot \mathbf{b}_q = 2\pi \delta_{pq}$ ($p, q = 1, 2$). Hence to the square lattice of primitive vectors $\mathbf{a}_1 = (a, 0)$ and $\mathbf{a}_2 = (0, a)$ considered the derived reciprocal-lattice primitive vectors became $\mathbf{b}_1 = (2\pi/a, 0)$, and $\mathbf{b}_2 = (0, 2\pi/a)$.

The oscillator displacements are treated in the Fourier space with only $\mathbf{G} = \mathbf{0}$, in the Floquet-Bloch form $w_j(\mathbf{R}) = W_j e^{-i\mathbf{k}\cdot\mathbf{R}}$. The periodic expansion with the Floquet-Bloch condition above mentioned to $w(\mathbf{r})$ also imposes the condition:

$$w(\mathbf{r} + \mathbf{R}) = w(\mathbf{r}) e^{-i\mathbf{k}\cdot\mathbf{R}}, \quad (8)$$

which in particular gives: $w(\mathbf{R}) = e^{-i\mathbf{k}\cdot\mathbf{R}} \sum_{\mathbf{G}} W_{\mathbf{G}}$. Hence, by employing the above conditions and the Fourier expansion to the delta function¹, the sum of forces on the plate, seen in the Eq(1), can be rewritten as:

$$\begin{aligned} \sum_R \sum_{j=1}^{N_o} f_j(\mathbf{R}) \delta(\mathbf{r} - \mathbf{R}) &= \sum_{j=1}^{N_o} k_j \left(\sum_{\mathbf{G}} W_{\mathbf{G}} - W_j \right) e^{-i\mathbf{k}\cdot\mathbf{r}} \sum_R \delta(\mathbf{r} - \mathbf{R}) \\ &= \sum_{j=1}^{N_o} k_j \left(\sum_{\mathbf{G}} W_{\mathbf{G}} - W_j \right) \frac{1}{S} \sum_{\mathbf{G}} e^{-i(\mathbf{k}+\mathbf{G})\cdot\mathbf{r}} \end{aligned} \quad (9)$$

Finally, substituting Eqs. (4),(5),(6), (8) and (9) into Eq. (1) gives to each Fourier component of displacement responses the following set of linear equations in terms of each vector G used in the Fourier expansion and to each \mathbf{k} wave vector considered in the reciprocal space:

$$\begin{aligned} \rho I_p \omega^2 \Psi_{x,\mathbf{G}} &= \frac{D}{2} \left\{ (1-\nu) [(k_x + G_x)^2 + (k_y + G_y)^2] \Psi_{x,\mathbf{G}} + (1+\nu) [(k_x + G_x)(k_y + G_y) \Psi_{y,\mathbf{G}} + (k_x + G_x)^2 \Psi_{x,\mathbf{G}}] \right\} \\ &\quad + \kappa_1^2 Gh [i(k_x + G_x) W_{\mathbf{G}} + \Psi_{x,\mathbf{G}}] \end{aligned} \quad (10)$$

$$\begin{aligned} \rho I_p \omega^2 \Psi_{y,\mathbf{G}} &= \frac{D}{2} \left\{ (1-\nu) [(k_x + G_x)^2 + (k_y + G_y)^2] \Psi_{y,\mathbf{G}} + (1+\nu) [(k_x + G_x)(k_y + G_y) \Psi_{x,\mathbf{G}} + (k_y + G_y)^2 \Psi_{y,\mathbf{G}}] \right\} \\ &\quad + \kappa_1^2 Gh [i(k_y + G_y) W_{\mathbf{G}} + \Psi_{y,\mathbf{G}}] \end{aligned} \quad (11)$$

$$\begin{aligned} \rho h \omega^2 W_{\mathbf{G}} &= Gh \kappa_1^2 \left\{ [(k_x + G_x)^2 + (k_y + G_y)^2] W_{\mathbf{G}} - i[(k_x + G_x) \Psi_{x,\mathbf{G}} + (k_y + G_y) \Psi_{y,\mathbf{G}}] \right\} \\ &\quad - \sum_{j=1}^{N_o} \frac{k_j}{S} \sum_{\mathbf{G}} W_{\mathbf{G}} + \sum_{j=1}^{N_o} \frac{k_j}{S} W_j \end{aligned} \quad (12)$$

$$-\omega^2 m_j W_j = k_j \sum_{\mathbf{G}} W_{\mathbf{G}} - k_j W_j \quad (13)$$

these equations can be expressed in the matrix form:

$$\begin{aligned} &\begin{pmatrix} [\mathbf{S}]_{11N \times N} & [\mathbf{S}]_{12N \times N} & [\mathbf{S}]_{13N \times N} & [\mathbf{0}]_{N \times N_o} \\ [\mathbf{S}]_{21N \times N} & [\mathbf{S}]_{22N \times N} & [\mathbf{S}]_{23N \times N} & [\mathbf{0}]_{N \times N_o} \\ [\mathbf{S}]_{31N \times N} & [\mathbf{S}]_{32N \times N} & [\mathbf{S}]_{33N \times N} + S^{-1} [\mathbf{K}_r]_{N \times N} & S^{-1} [\mathbf{K}_r']_{N \times N_o} \\ [\mathbf{0}]_{N_o \times N} & [\mathbf{0}]_{N_o \times N} & -[\mathbf{K}_r']_{N_o \times N} & [\mathbf{K}_d]_{N_o \times N_o} \end{pmatrix} \cdot \begin{pmatrix} \Psi_{x,\mathbf{G}} \\ \Psi_{y,\mathbf{G}} \\ W_{\mathbf{G}} \\ W_j \end{pmatrix} \\ &= \omega^2 \begin{pmatrix} \rho I_p [\mathbf{I}]_{N \times N} & [\mathbf{0}]_{N \times N} & [\mathbf{0}]_{N \times N} & [\mathbf{0}]_{N \times N_o} \\ [\mathbf{0}]_{N \times N} & \rho I_p [\mathbf{I}]_{N \times N} & [\mathbf{0}]_{N \times N} & [\mathbf{0}]_{N \times N_o} \\ [\mathbf{0}]_{N \times N} & [\mathbf{0}]_{N \times N} & \rho h [\mathbf{I}]_{N \times N} & [\mathbf{0}]_{N \times N_o} \\ [\mathbf{0}]_{N_o \times N} & [\mathbf{0}]_{N_o \times N} & [\mathbf{0}]_{N_o \times N} & [\mathbf{m}_d]_{N_o \times N_o} \end{pmatrix} \cdot \begin{pmatrix} \Psi_{x,\mathbf{G}} \\ \Psi_{y,\mathbf{G}} \\ W_{\mathbf{G}} \\ W_j \end{pmatrix} \end{aligned} \quad (14)$$

The Eq (14) represents an usual eigenvalue problem for ω^2 after a left multiplication of the inverse of inertial matrix, seen at the right hand side of the equation. It can be solved to each Bloch vector \mathbf{k} in the irreducible region of the first Brillouin Zone, resulting in $3N + N_o$ eigenvalues, ω^2 , which are used to represent the dispersion relation related to the band structure (BS), $\omega(k)$. The absence of a range of eigenvalues, $\omega(k)$, to the swept range of \mathbf{k} wave-vectors of propagating waves, are seen as band gaps in the BS.

¹ $\sum_{\mathbf{R}} \delta(\mathbf{r} - \mathbf{R}) = \sum_{\mathbf{G}} \frac{1}{S} e^{-i\mathbf{G}\cdot\mathbf{r}}$, in which S is the area of the unit cell associated with the periodic lattice: $S = |\mathbf{a}_1 \times \mathbf{a}_2|$

2 SIMULATED EXAMPLE

2.1 Dispersion Curve

In this section, it is presented a simulated example of wave band gaps calculated with a metamaterial thick plate (Reissner-Mindlin theory). Results are also compared with the ones obtained by a bare plate (a plate without resonators but with the same mass density) and a metamaterial thin plate (Kirchhoff-Love theory). For this simulation, a thickness of the plate is $h = 0.002$ m. In this example it was consider: only a single array of resonators ($N = 1$ and $\mathbf{r}_1 = 0$) attached in a square unit-cell with a lattice constant ($a = 0.008$ m), much smaller than the flexural wave length of the host plate. The natural frequency of the resonator was tuned according to the result of the numerical simulation of modal analysis for the first mode of cell flexural; and the geometric parameters and material properties of the metamaterial plate are listed in Table 1:

Table 1 – Metamaterial plate geometric parameters and material properties.

Parameters	Values
Mass density (ρ)	800 kg/m ³
Young's modulus (E)	1.8 GPa
Structural loss factor (η_p)	0.02
Poisson's ratio (ν)	0.39
Plate thickness (h)	0.002 m
Lattice parameter (a)	6.4×10^{-5} m ²
Unit cell area for square lattice ($S = a^2$)	0.008 m
Resonator to plate mass ratio (γ)	0.883
Resonator loss factor (η_r)	0.02
Resonator natural frequency (f_r)	1253 Hz

The Figure 2a) shows the dispersion diagram comparison of bare plate and metamaterial plate calculated by PWE with Kirchhoff-Love (K-L) theory (Xiao,2012f) and the corresponding bare plate and metamaterial plate calculated by PWE with Reissner-Mindlin (R-M) theory Eq. (1). As expected for both plates as the frequency range increases the band structure of metamaterial thick and thin plates starts to diverge. It comes from the R-M's thick plate theory which take into account shearing of cross sections and rotational inertia not included in K-L's theory. At high frequencies, the shear resistance terms become dominant, so that the flexural wave equation simplifies to the shear wave equation. Figure 2b) shows the local resonator band gap at the frequency $f_r = 1253$ Hz.

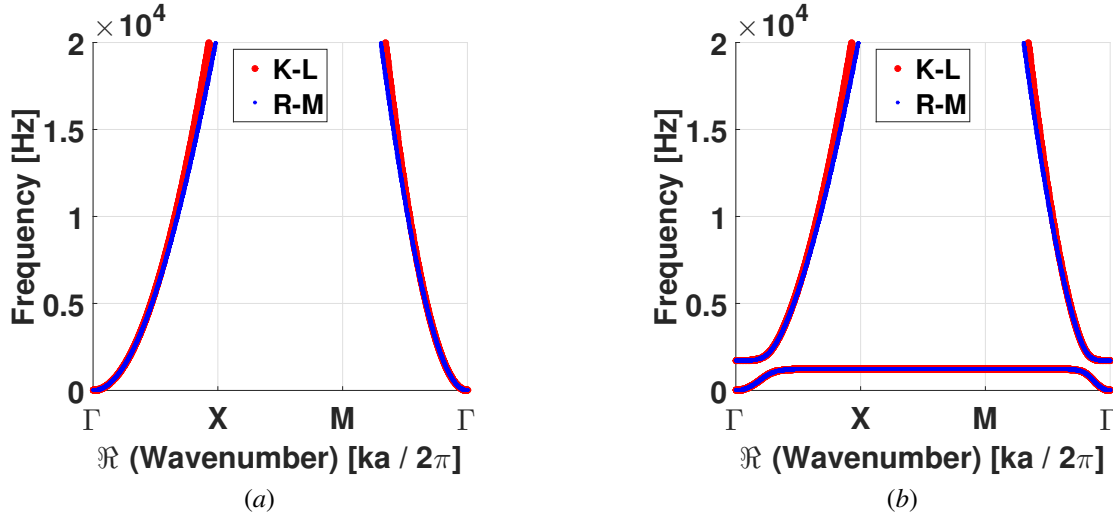


Figure 2 – Dispersion diagram comparison of (a) bare plates and (b) metamaterial plates using PWE with Kirchhoff-Love (K-L) and Reissner-Mindlin (R-M) theories.

2.2 Numerical results

In this section it is presented a metamaterial thick plate with spatial periodic distribution with local resonators. In this structure, we want to demonstrate the influence of the band gap in structural dynamic behavior. The objective is to compute the modal analysis and the forced response of the EM thick plate and then, compare these results with the dispersion curve obtained using the PWE method. For this simulation a commercial finite element analysis software

ANSYS (Mechanical APDL Release 18.1) was used. The EM thick plate is modelled with ANSYS using an appropriated element type from its element library, *i.e.*, a 3D solid element (SOLID187). The global system is modelled using a free mesh with 1690 triangular elements (3D) for only one cell and 69994 triangular elements (3D) for whole plate as shown Figure 3a) and Figure 3b) respectively.

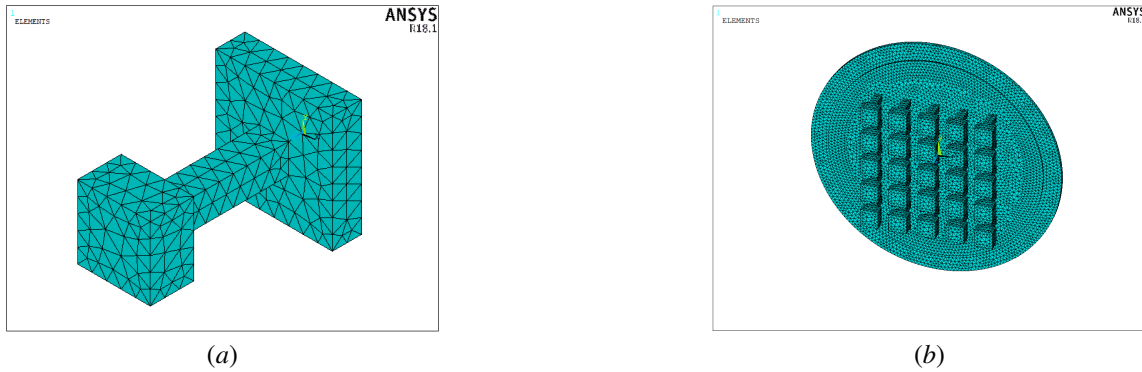


Figure 3 – FE model of the EM thick plate (a) Only a cell with resonator (b) Whole plate.

For the boundary conditions of the cell with the resonator the edges are clamped, whereas the whole thick plate are free edges. The Figure 4 illustrates the modal analysis of the cell and the whole EM thick plate using FE.

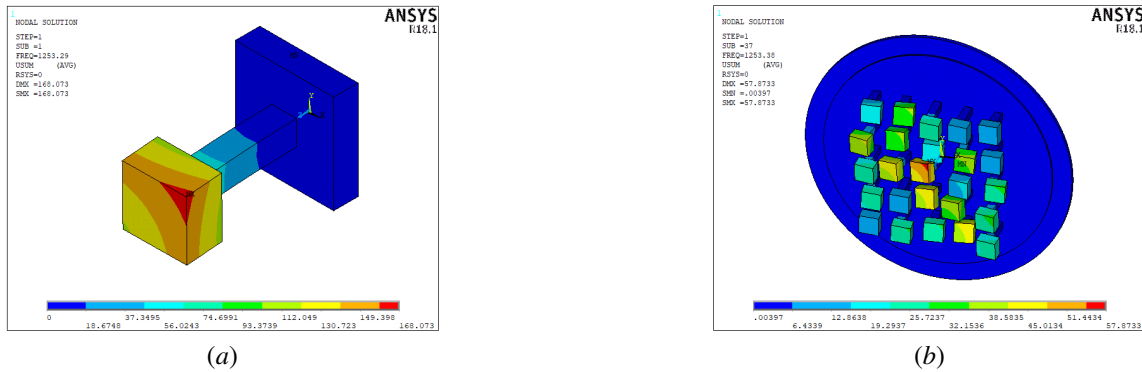


Figure 4 – Modal analysis of EM thick plate (a) Only a cell with resonator (b) Whole plate.

In Figure 4 it is illustrated the flexural modes a) z_x in 1253.29 Hz and b) z_x in 1253.38 Hz. In Figure 4b) we can observe that resonators absorb most of plate vibration in this frequency. For a better understanding of the comparison of the dispersion curve obtained by the PWE method and transmittance between the amplitudes of different points of the plate through the analysis of the forced response by finite elements, Figure 5 presents two modes of flexural vibration of plate :

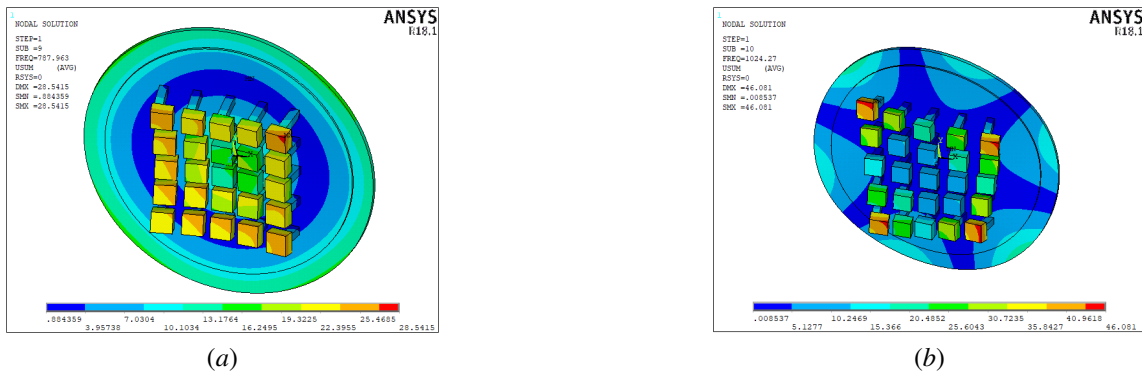


Figure 5 – Modal analysis of EM thick plate (a) z_x in 787.96 Hz (b) z_x in 1024.27 Hz.

Based on the results of the Figure 5 obtained by the modal analysis of the flexural modes of the plate with resonator, we calculated the transmittance among the FRFs in excitation and displacement of the structure and compared the transmittance calculated by FE and the real Bloch wave vectors obtained from PWE formulated from 0 Hz up to 2000 Hz.

For PWE calculation, we consider one attached periodic arrays of 1-DOF resonators with 1253 Hz, this frequency was obtained from modal analysis in Figure 4a), material properties from Table 1.

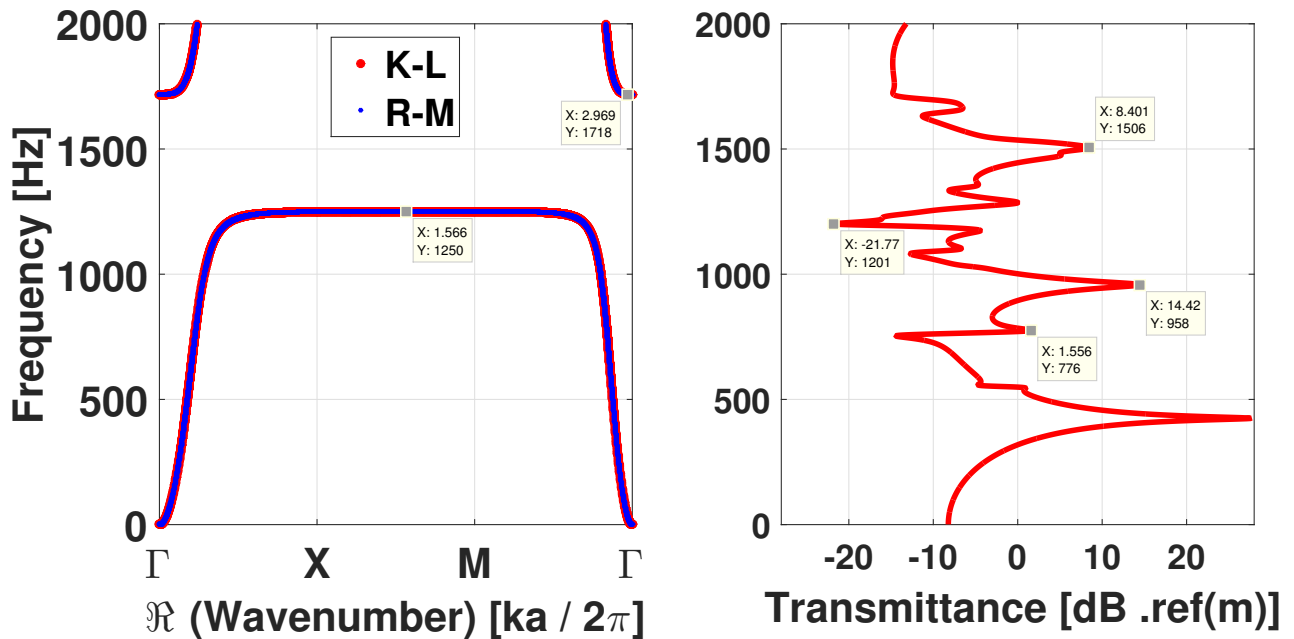


Figure 6 – Comparison of real values of Bloch wave vector calculated by PWE and transmittance computed by FE.

3 CONCLUSIONS

We investigated the flexural wave propagation and vibration transmission in a LR thick plate with a 2D periodic array of attached spring-mass resonators. Through the PWE method, the necessary matrix formulation was deduced for the calculation of Bloch wave vectors to which it was used to calculate the wave attenuation performance of band gaps. We use the finite element method to calculate the vibration transmittance in thick plate. According to the Figure 6 we can observe that the dispersion curve shows a bandwidth between 1250 and 1720 Hz. Within this frequency range observed in the dispersion curve, we can observe that the attenuation effect of the flexural vibration of the plate is achieved by adjusting the frequency of the structural resonator inserted in the plate, because near this region the observed transmittance has the lowest value. Another important analysis to be discussed is that although in the band gap region there should be no propagating waves in the structure (only evanescent waves), other modes of vibration may be observed.

ACKNOWLEDGMENTS

The authors would like to acknowledge the Brazilian research funding agency CNPq (National Council for Scientific and Technological Development) for its financial support to this research.

REFERENCES

- Brillouin53 Brillouin, L., “Wave Propagation in Periodic Structures”, Dover, New York, 2nd edition, 1953.
- Hambric Hambric, S., Sung, S., Nefske, D., “Engineering Vibroacoustic Analysis (Methods and Applications), Wave-based Structural Modeling”, John Wiley & Sons, 2016.
- Liu2000 Liu, Z., Zhang, X., Mao, Y., Zhu, Y.Y., Yang, Z. and Chan, C.T., “Locally resonant sonic materials”. Science, Vol. 289, 2000, pp. 1734.
- Mindlin Mindlin, R., “Thickness Shear and Flexural Vibrations of Crystal Plates”, Journal of Applied Physics, v.22,n.3,1951, pp.316-323
- Norris Norris, A., “Flexural waves on narrow plates”, The Journal of the Acoustical Society of America, v.113,n.5,2003, pp.2647-2658.
- Oudich2010 Oudich, M., Li, Y., Assouar, B.M. and Hou, Z., “A sonic band gap based on the locally resonant phononic plates with stubs”, New Journal of Physics, 12, 083049, 2010.
- Sigalas92 Sigalas, M.M. and Economou, N.M., “Elastic and acoustic wave band structure”, Journal of Sound and Vibration, 158(2), 1992, pp. 377-382.

- Sigalas94 Sigalas, M.M. and Economou, N.M., "Elastic waves in plates with periodically placed inclusions", *J. Appl. Phys.*, 75 (6), 1994, pp. 2845-2850.
- Szilard Szilard, R. "Theories and applications of plate analysis: classical, numerical and engineering methods", John Wiley & Sons, New Jersey, 2004.
- Xiao2012f Xiao, Y., Wen, J., Wen, X., "Flexural wave band gaps in locally resonant thin plates with periodically attached springmass resonators", *Journal of Physics D: Applied Physics*, v.45, no.19, 2012, pp.1-1
- Xiao2012s Xiao, Yong., Wen, Jihong., Wen, Xisen., "Sound transmission loss of metamaterial-based thin plates with multiple subwavelength arrays of attached resonators", *Journal of Sound and Vibration*, 331(25), 2012, pp. 5408-5423.